

Variable Trust Setting for Safe and Ethical Algorithms for Navigation of Autonomous Vehicles (C-NAV) on a Highway

Joshua D'Souza, Jisun Kim and James E. Pickering
College of Engineering and Physical Science, Aston University, U.K.

Keywords: Control Engineering, Autonomous Vehicles, Model-Predictive Control (MPC), Navigation Algorithms, Ethics, Vehicle Safety.

Abstract: This paper presents the use of an ethical model-to-decision approach for promoting safe manoeuvrability of autonomous vehicles (AVs) on highways, when considering scenarios such as exiting a highway via a slip road. In this research, a modelling and simulation approach is undertaken. The modelling involves the use of an adaptive model-predictive control (MPC) algorithm with a dynamic bicycle model. The approach was developed to incorporate a novel continuous evaluation of the distances between AVs (considering virtual boundaries), logical sequences towards achieving safe lane change and slip road exit manoeuvres (driving rules based on deontological ethics), and control logic towards accounting for acceleration, deceleration, and constant velocity. Based on this, a novel continuous risk assessment algorithm has been developed based on the product of collision probability and harm. This has been used to investigate the introduction of a novel trust setting that gives the user 'control' of how the AV operates around other AVs. The results presented in the paper highlight the effectiveness of the approach, i.e., the ability to undertake ethical and safe manoeuvres in the event of difficult highway decision scenarios such as slip road exits.

1 INTRODUCTION

In recent years there have been significant developments in the field of autonomous vehicles (AVs). Recent improvements in communication technology and computational power have meant that AVs are now a possibility in the future to enhance safety and improve efficiency of operation when compared to human-driven vehicles (HDVs), see (Bajpai, 2016) and (Taibat, et al., 2018). However, the replacement of HDVs with AVs on the roads introduces questions regarding how they should act in given scenarios, e.g., performing a lane change to exit at a junction. For example, should the AV perform manoeuvres in a selfish manner to minimise journey time? It is considered that such an approach would increase the risk of a collision. Or should the AV operate based on 'if' and 'then' commands in a respectable manner to other road users? This approach is typical of the behaviour of a human operator of a vehicle, resulting in minimising the risk of a collision. Such a scenario introduces questions of just how an AV should be programmed. These questions involve the investigation of safety and ethical considerations, thus ensuring that AV

navigation planning decisions are justifiable and reasonable. With the transition from HDVs to autonomous driving, safety validation of the intended functionality now becomes a key challenge due to the uncertainty of the driving environment, see (Pettersson and Karlsson, 2015). Simulations can be used to explore novel navigation algorithms as they are safer and less expensive, see (Koopman and Wayner, 2016) and (Kalra and Paddock, 2016). Determining how an AV will perform in simulation is an important step as it enables different navigation algorithms to be explored and any potential defects to be highlighted and considered at the design stage.

In this paper, simulation tools will be used to investigate the deontological ethical principles of Immanuel Kant for AV navigation on a highway, with the initial approach being developed by the authors, see (Pickering et al., 2018), (Gilbert et al., 2021) (D'Souza, Burnham and Pickering, 2022) and (Pickering and D'Souza, 2023). In this paper, further considerations will be given to developing a novel continuous evaluation risk tool for highway driving. This is based on estimating the collision probability and harm, in a similar manner to the approach developed in (Geisslinger, Poszler and Lienkamp,

2023). In the paper by Geisslinger et al., 2023, the authors developed novel trajectory planning algorithms based on the EU commission expert groups ‘20 recommendations’, with the aim of the research being to fairly distribute risk amongst the road users in the immediate vicinity. As part of this, the authors developed a risk evaluation tool for driving scenarios (note that the highway scenario was not considered in their research). In (Németh, B., 2023), the author has developed a coordinated control approach using model predictive control (MPC) for ethical manoeuvres of AVs – a similar approach is used in this research.

The research in this paper is based on work undertaken on the Safe and Ethical Algorithms for Navigation of Autonomous Vehicles (C-NAV) project and aims to support the Research Strategy (published 19 August 2022) by the UK Government, (Responsible Innovation in Self-Driving Vehicles, 2022).

2 BASELINE MODEL

A dynamic bicycle model is incorporated to represent an AVs motion within the constructed coordinate framework, see Figure 1. The two vectors denoted V_x and V_y represent the longitudinal and lateral velocities, respectively. The path followed by the AV depends on a reference trajectory denoted Y_{ref} . The reference trajectory is generated by setting the input as the steering angle, denoted δ . The two variables, lateral position, denoted Y_{ref} and yaw angle reference, denoted φ_{ref} are determined with respect to the horizontal axis, denoted X – axis, ψ denotes the yaw angle, l_f denotes the longitudinal distance from the center of gravity to the front tyres and l_r denotes the longitudinal distance from the centre of gravity to the rear tyres.

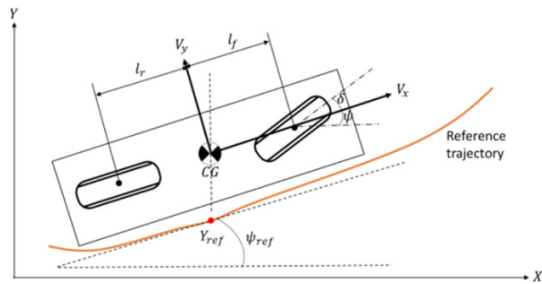


Figure 1: Reference trajectory control of a dynamic bicycle mode.

2.1 Adaptive Model Predictive Control

An adaptive MPC algorithm is used, see Figure 2. For brevity, details of the adaptive MPC and the model parameters are not given in this paper. However, full details can be found in (Melda, 2023). For the adaptive MPC, a dynamic state-space bicycle model adopted from (Rajamani, 2011) is given by the following form:

$$\frac{d}{dt} \begin{bmatrix} \dot{y} \\ \psi \\ \dot{\psi} \\ Y \end{bmatrix} = A \begin{bmatrix} \dot{y} \\ \psi \\ \dot{\psi} \\ Y \end{bmatrix} + \begin{bmatrix} \frac{2C_f}{m} \\ 0 \\ \frac{2l_f C_f}{I_z} \\ 0 \end{bmatrix} \delta \quad (1)$$

where,

$$A = \begin{bmatrix} -\frac{2C_f+2C_r}{mV_x} & 0 & -V_x - \frac{2C_f l_f - 2C_r l_r}{mV_x} & 0 \\ 0 & 0 & 1 & 0 \\ \frac{2l_f C_f - 2l_r C_r}{I_z V_x} & 0 & -\frac{2l_f^2 C_f + 2l_r^2 C_r}{I_z V_x} & 0 \\ 1 & V_x & 0 & 0 \end{bmatrix}$$

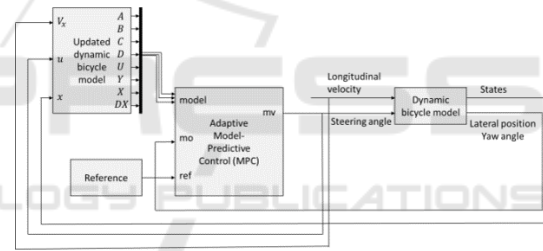


Figure 2: Adaptive model predictive control (MPC).

Considering the input to the system to be the steering angle, the objective of adaptive MPC is to minimise the deviation of the lateral displacement and the yaw angle of the AV. Considering vehicle performance and passenger comfort, the maximum steering angle and steering rate are capped at 30 degrees and 15 degrees per second, respectively.

2.2 Highway Scenario

In this section, a two-axis coordinate system is used for the highway, see Figure 3. The AVs on the highway are denoted AV_a and AV_b , with these located in Lanes 1 and 2, respectively, V_a and V_b denote the respective resultant velocities, (x_a, y_a) and (x_b, y_b) denote the lateral and longitudinal positions measured from origin $(0, 0)$, respectively.

In this paper, the highway scenario is given in Figure 4, with the corresponding way points for AV_a

and AV_b (further details regarding the simulation are given in later sections), where AV_a remains in Lane 1 and AV_b performs an overtake manoeuvre on AV_a to enable exit at the slip road.

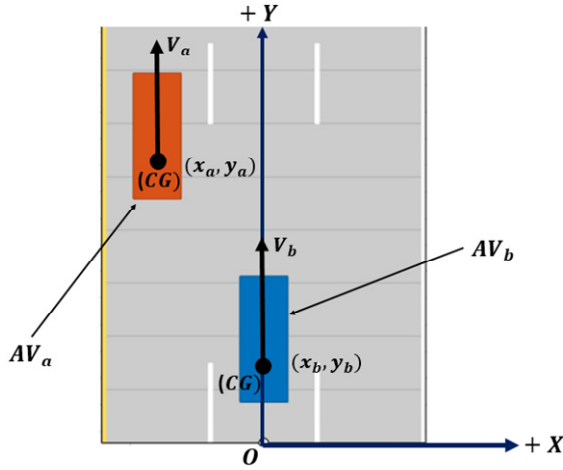


Figure 3: Two-dimensional coordinate system of the highway setup.

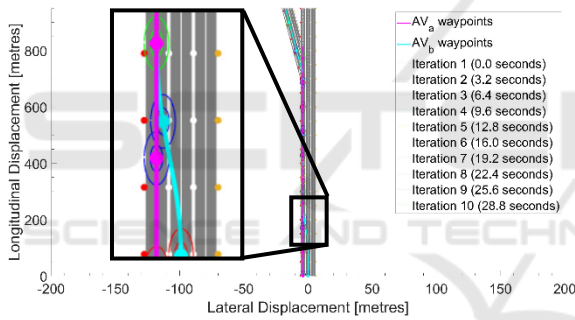


Figure 4: Highway scenario with each of the autonomous vehicle's (AV's) waypoints.

3 RISK ASSESSMENT

In this Section, a collision risk assessment model is developed to quantify the risk associated with the interaction between the two AVs. The risk assessment is given by Equation (2):

$$R_a = P(c) H_l \quad (2)$$

where R_a denotes the risk assessment, which is continuously updated during the simulation, $P(c)$ denotes the probability of a collision and H_l denotes the harm index. Further details regarding Equation (2) are given in the following sections. The risk assessment is set-up such that a value of 0 corresponds to a risk-free situation and a value of 1

corresponds to a high-risk situation, i.e., high likelihood of a collision event.

3.1 Virtual Boundaries

To ensure safe manoeuvrability of the AVs, use is made of 'barrier' and 'buffer' virtual boundaries. The barrier zone is denoted B_a and the buffer zone is denoted B_u , see Figure 5. The barrier of each AV must not be entered by another AV. However, the buffer of each AV can be entered but it must be left as soon as possible. The boundaries are set up on each AV from their centre of gravity (CG) such that the barrier length, denoted l_{B_a} , spans out from $l_{B_{a_f}}$ and $l_{B_{a_a}}$ from the fore (front) and aft (rear) directions of the AVs heading, respectively, and between $l_{B_{a_l}}$ and $l_{B_{a_r}}$ from the left to the right of the AV, respectively. The following values are used for the barrier: $l_{B_{a_f}} = 10m$, $l_{B_{a_a}} = 10m$, $l_{B_{a_l}} = 1m$ and $l_{B_{a_r}} = 1m$. The buffer length, denoted l_{B_u} similarly spans out at distances of $l_{B_{u_f}}$, $l_{B_{u_a}}$, $l_{B_{u_l}}$ and $l_{B_{u_r}}$ from the centre of gravity for the fore, aft, left and right of the AV's heading, respectively. The following values are used for the buffer: $l_{B_{u_f}} = 20m$, $l_{B_{u_a}} = 20m$, $l_{B_{u_l}} = 2m$ and $l_{B_{u_r}} = 2m$.

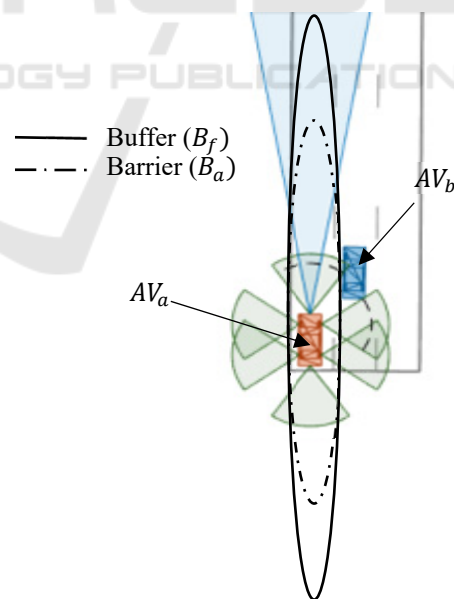


Figure 5: Virtual boundary of an autonomous vehicle (AV).

3.2 Collision Probability

For two AVs in motion, the probability of a collision, denoted $P(c)$, is dependent on the longitudinal

separation distance, denoted Δy_s , and lateral separation distance, denoted Δx_s between the two vehicles, i.e.,

$$P(c) = f(\Delta x_s, \Delta y_s) \quad (3)$$

If the virtual boundaries are respected (i.e., no overlap of their respective barriers), the probability of a collision is 0. To this extent, the initial values for the barrier virtual boundaries are set up for the risk assessment model for each AV that are considered to be safe, i.e., $\Delta x_{safe} = 4m$ (considering the sides of the two AVs) and $\Delta y_{safe} = 40m$ (considering the front and rear of each AV), where Δx_{safe} and Δy_{safe} denote safety benchmark values for lateral and longitudinal separation between two AVs, respectively.

On this basis, the probability of a collision can be derived to be proportional to the ratio of the measured separation distances to their respective benchmark values. Hence, the following equation can be derived as the collision probability calculation for the developed risk assessment model:

$$P(c) = \left[1 - \frac{\Delta x_s}{\Delta x_{safe}} \right] \left[1 - \frac{\Delta y_s}{\Delta y_{safe}} \right] \quad (4)$$

3.3 Collision Harm Index

In addition to calculating collision probabilities, another important factor that defines the severity of a potential collision involves mapping the potential harm that is associated with a given action. In this section, harm is quantified by the collision energy in each scenario. This is modelled by considering the law of conservation of momentum and energy for a two-vehicle inelastic collision, with these being given by:

$$m_{AV_a} v_{AV_a} + m_{AV_b} v_{AV_b} = m_c v_f \quad (5)$$

where m_{AV_a} and m_{AV_b} denote the masses of AV_a and AV_b , respectively, v_{AV_a} and v_{AV_b} denote the collision velocities of AV_a and AV_b , respectively. Considering the post-collision AV properties, m_c denotes the combined AV masses and v_f denotes the final velocity of the combined AVs. Based on Equation (5), the conservation of energy for an inelastic two-vehicle collision is given by:

$$\begin{aligned} \frac{1}{2} m_{AV_a} v_{AV_a}^2 + \frac{1}{2} m_{AV_b} v_{AV_b}^2 \\ = \frac{1}{2} (m_{AV_a} + m_{AV_b}) v_f^2 \\ + \Delta E \end{aligned} \quad (6)$$

where ΔE denotes the collision energy between the two AVs. Based on Equation (6), the Harm Index is derived, and is given by:

$$H_I = \frac{\Delta E_{actual}(t)}{\Delta E_{max}} \quad (7)$$

where ΔE_{actual} denotes the actual collision energy between the two AVs and ΔE_{max} denotes the maximum possible collision energy between the two AVs. The Harm Index is dimensionless where the values vary between 0 and 1, where 0 corresponds to a collision that would cause the least harm under the given circumstance, i.e., the least possible collision energy. A value of 1 corresponds to the collision that would result in the greatest amount of harm, i.e., the highest possible collision energy. In this case, since the mass of the AVs are constant, ΔE_{max} depends on the maximum possible velocity at which the overtaking vehicle can travel at on the highway, i.e., 70 mph (or alternatively 31.29 m/s).

4 SIMULATION SET-UP

This section details the mathematical considerations required to achieve the desired driving manoeuvres whilst incorporating the safe and ethical conditions.

4.1 Lane Change

In this case, AV_b is considering a lane changing manoeuvre to position itself in front of AV_a . Considering the driving rules and the virtual boundaries, a lane change is a direct result of always maintaining respect of the boundary zones, see (Pickering and D'Souza, 2023). This requires a continuous evaluation of both AVs. To mathematically capture such requirements, the following equations describe the longitudinal, lateral, and resultant separation distances:

$$y_s = y_b - y_a \quad (8)$$

$$x_s = x_b - x_a \quad (9)$$

$$R_s = \sqrt{(y_s^2 + x_s^2)} \quad (10)$$

where y_s denotes the longitudinal separation between the two AVs, x_s denotes the lateral separation between the two AVs and R_s denotes the resultant separation. Maintaining the same objective of respecting the boundaries, it is therefore desired that there are no overlaps between the boundaries of the two AVs. This is achieved with consideration of the following:

$$y_b(t + \Delta t) = y_a(t + \Delta t) + l_{B_{af}AV_a} + l_{B_{aa}AV_b} \quad (11)$$

$$y_s > l_{B_{af}AV_a} + l_{B_{aa}AV_b} \quad (12)$$

where t denotes the time, Δt denotes the time required to complete a lane change, $l_{B_{af}AV_a}$ denotes the front portion of AV_a barrier and $l_{B_{aa}AV_b}$ denotes the aft (rear) portion of AV_b barrier. Equation (11) is derived such that AV_b clears the barrier of AV_a after the lane change is achieved, whilst maintaining the respect of the boundaries longitudinally; with this forming the lane change Constraint 1. Equation (12) is adopted to ensure that the boundaries are not violated laterally at the start and during the phase of the lane changing manoeuvres. Hence, AV_b is constrained to initiating the manoeuvre only when a longitudinal separation of the sum of the front portion of AV_a 's barrier and the rear portion of AV_b barrier, with this forming the second constraint for a 'safe' lane change.

4.2 Slip Road Entry

This section will detail the constraints in place for the slip road exit. Considering the driving rules and the virtual boundaries, the first slip road entry (i.e., exiting the highway) constraint involves AV_b longitudinal displacement of 700 m. To further enhance the safety aspects, it is important to ensure that AV_b does not undertake any dangerous actions, i.e., suddenly changing directions without considering the virtual boundaries.

4.3 Adaptive Velocity Control

For AV_b to be able to perform the overtaking move into Lane 1 ahead of AV_a , the velocities of the two AVs will need to be altered, i.e., AV accelerating or decelerating to increase or decrease velocity. This section details the modelling required to capture the AV 's acceleration and deceleration properties. A logical sequence is required to be implemented to establish when the AV needs to accelerate, decelerate, or maintain a constant velocity. MATLAB Stateflow logic is used for this, see Figure 6. The inputs to the logic are the lateral position of AV_b , individual longitudinal displacements of both AV_s , and the longitudinal separation between the two AVs. The Stateflow chart is defined for AV_b to initially accelerate to 31.29 m/s (70mph) from its starting velocity. This

is then maintained until a safe lane change has occurred alongside a safe slip road entry, with the AV then decelerating to the initial velocity. This results in a 4-stage velocity control process involving: acceleration, constant velocity, deceleration, and constant velocity.

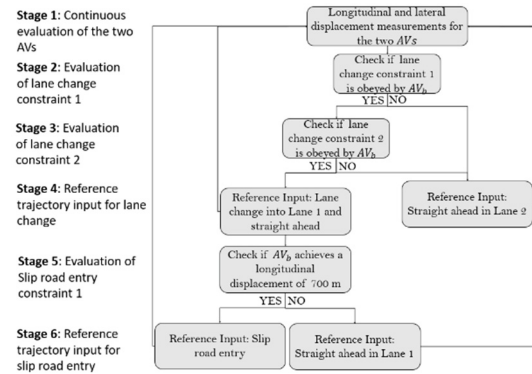


Figure 6: Flowchart illustrating control logic of an adaptive velocity control.

4.4 Simulation Logic

Figure 7 illustrates a flowchart containing the AVs decision making logic/algorithm. The logic is set up to comprise of 6 major stages, with these being:

- i. Stage 1 involves the incorporation of longitudinal and lateral displacements of the two AVs, involving continuous evaluation of the two-vehicles relative displacement.
- ii. Stage 2 is setup to test the validity of the first lane change constraint, determining whether virtual boundaries would be respected after the lane change manoeuvre. If obeyed, this builds onto Stage 3.
- iii. Stage 3 tests the validity of lane change Constraint 2. A negative result from Stage 3 deems this to be an 'unsafe' lane change manoeuvre.
- iv. Conversely, achieving the constraint set in Stage 3 results in ensuring that a safe lane changing manoeuvre can be undertaken, leading to the input of the lane change reference trajectory in Stage 4, placing AV_b in lane 1, i.e., Constraint 2 for a safe slip road entry.
- v. Stage 5 undertakes a comparison study, determining whether a longitudinal displacement of 700 m is achieved, i.e., longitudinal location of the slip road. If the comparison study is positive, a slip road entry is deemed to be safe, which results in the slip road entry reference trajectory input.
- vi. Procedure successful.

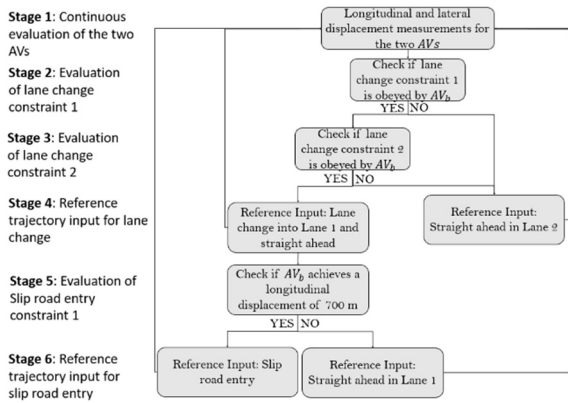


Figure 7: Flowchart illustrating the simulation logic.

5 RESULTS

A scenario is detailed in this section to highlight the operation of the developed algorithms.

5.1 Deontological Ethics Example

The scenario in the results section is set such that both AVs (i.e., AV_a and AV_b) are of equal masses and start off at the same longitudinal displacement and initial velocity, as detailed in Table I. Table I also details the initial lateral displacement, initial lane position and the desired lane position.

Table 1: Input parameters for scenario 1.

	AV_a	AV_b
Mass [kg]	1575	1575
Initial velocity [mph]	60	60
Initial longitudinal displacement [m]	0	0
Initial longitudinal displacement [m]	-4	0
Initial lane position	Lane 1	Lane 2
Desired lane position	Lane	Lane 1 and slip road entry

The adaptive MPC algorithm presented in Section 2.2 is now simulated with the properties given in Table I. The initial results of this section are also given in an earlier paper published by the authors, see (Pickering, D'Souza, 2023). Initially two AVs are simulated using way points given in Figure 4. For the simulation, AV_a in the left-hand lane will travel at a constant velocity of 60 mph (26.82 m/s). The velocity of the overtaking AV (i.e., AV_b) will alter based on obeying the driving ethical rules are obeyed,

such that AV_b does not enter the 'barrier' virtual boundary of AV_a . Figure 4 also illustrates the highway simulation scenario of the two AVs, with the way points and the 10 corresponding iterations of the simulation, i.e., from 0 seconds to 28.8 seconds.

5.2 Risk Assessment Example

A simulation is now given using the scenario detailed in Section 5.1 involving the risk assessment. However, in this example the reference trajectory input (i.e., way points) for the adaptive MPC for a lane change manoeuvre (i.e., for AV_b) is applied. This change is applied to demonstrate a scenario whereby the risk assessment is used. For the example given in Section 5.1, this resulted in a peak risk assessment value of 0.23, i.e., both AVs are at low risk of a collision.

Figures 8 and 9 illustrate the lateral separation versus time and longitudinal separation versus time between the between AVs, respectively for the scenario given in Figure 4.

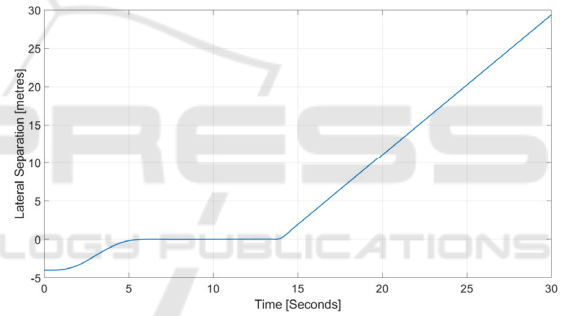


Figure 8: Deontological ethics initial results: lateral separation versus time for the two autonomous vehicles.

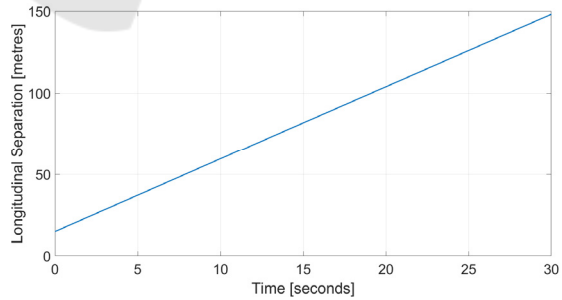


Figure 9: Deontological ethics initial results: longitudinal separation versus time for the two autonomous vehicles.

Considering the result obtained in Figure 4 (and the zoomed in area), AV_b performs a lane changing manoeuvre that results in the overlap of the virtual boundaries of the two AVs during that phase, i.e., the buffer zone. However, the barrier for each of the AVs

is respected. The result of the risk assessment for this scenario is given in Figure 10. In Figure 10, the journey initial starts off as a risk-free journey. However, based on the logic applied in the simulation, AV_b begins to perform the lane changing manoeuvre once the barrier zone is passed. However, this results in the AVs entering into one another's buffer zones. In Figure 10, the peak risk assessment (PRA) and duration of risk imposed (DRI) values are labelled, where values of 0.23 and 6.38 seconds are captured, respectively. The risk assessment does not last for a long duration due to the adaptive velocity control of AV_b , with this resulting in AV_b travelling at a velocity of 70mph when overtaking AV_a , and then returning to the initial velocity of 60mph once passed AV_a , see Figure 11.

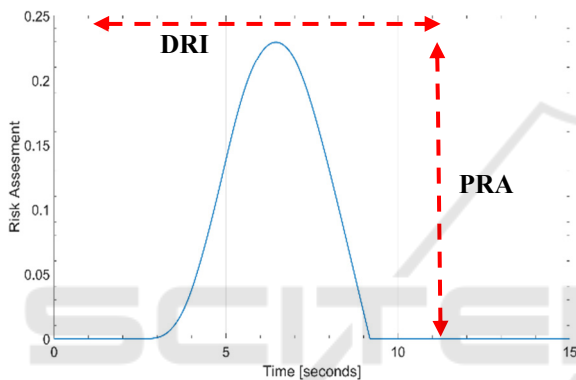


Figure 10: Graphical output illustrating the risk versus time generated.

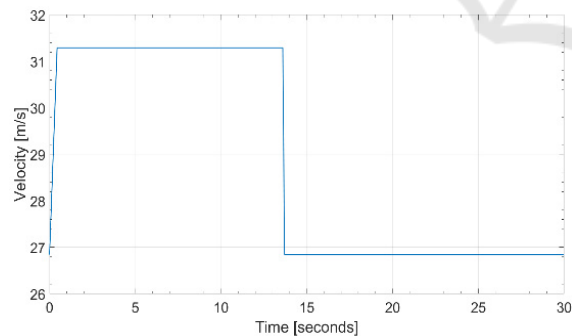


Figure 11: Adaptive velocity control output.

5.3 Variable Trust Setting

Trust is an important element for occupants of AVs due to the likelihood of entering into vulnerable situations whereby the occupant entrusts in the system (Körber, Baseler and Bengler, 2018). Trust can have an impact on the occupant's decision to use the automation (Lee and Moray, 1994). Trust is

defined as the “willingness of a party to be vulnerable to the actions of another party based on the expectation that the other will perform a particular action important to the trustor, irrespective of the ability to monitor and control that other party” (Mayer, Davis, and Schoorman, 1995). For there to be trust in the automation, the multifaceted construct that embraces performance, process, purpose, and foundation must be established. Performance is related to consistency, stability and desirability of automation. Process indicates operators' knowledge of the underlying algorithms that govern behaviour of the system. Purpose represents the producers' intention in creating the system (Lee and Moray, 1992).

Considering the risk assessment example in Section 5.2, this is now used in the development of a variable trust setting. A setting of 0% implies no trust in the AV technology and 100% implies complete trust in the AV technology, with this setting based on the user preference. Varying the level of trust of the AV will result in varying the distance of the barrier element of the virtual boundaries, with the values used in this paper given in Table II. Recall from Section 3.0 that another AV should not enter into another AVs barrier (an overtake will take place once the barrier has been passed).

The model is now used to investigate the effect of the variable trust settings given in Table II. Figure 12 illustrates the risk assessment results for a range of variable trust settings, where the PRA and DRI values are labelled. The key findings from Figure 12 relating to the PRA and DRI are given in Table III. Based on the findings, these are as expected, i.e., when the barrier length reduces the risk assessment (i.e., risk exposed to the occupants) increases.

Table 2: Variable trust setting in percentage and linguistic terms relating to the virtual boundaries.

Variable Trust Setting [0 – 100%]	Linguistic terms	Virtual Boundaries [m]	
		Barrier	Buffer
0	No trust	12	20
25	Little trust	11	20
50	Medium trust	10	20
75	Medium to high trust	9	20
100	Complete trust	8	20

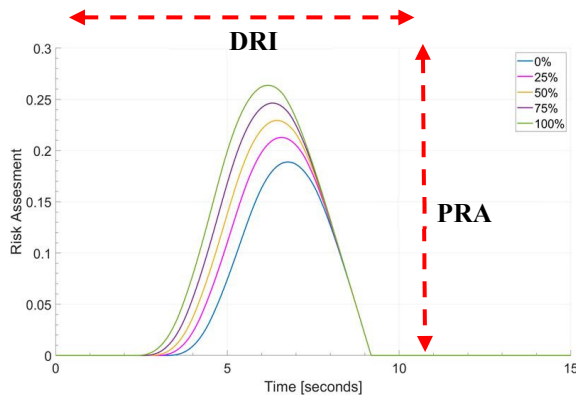


Figure 12: Longitudinal displacement versus time of the autonomous vehicle compared to the reference.

Table 3: Variable trust setting in percentage and the corresponding results for peak risk assessment (PRA) and duration of risk imposed (DRI).

Variable Trust Setting [0 – 100%]	Peak Risk Assessment (PRA)	Duration of Risk Imposed (DRI) [Seconds]
0	0.19	5.88
25	0.21	6.18
50	0.23	6.38
75	0.25	6.58
100	0.26	6.78

6 CONCLUSIONS AND FURTHER WORK

This paper has presented a novel approach towards enhancing safe and ethical manoeuvrability of autonomous vehicles (AVs) on highways. Regarding the safe and ethical decision-making strategies, the paper has considered driving rules with Maxims based on deontological ethics and coupled with the application of AV virtual boundaries. An adaptive model predictive control (MPC) algorithm alongside the incorporation of a dynamic bicycle model is used to model each AV and achieve the desired trajectories. The paper also proposes a novel methodology for a continuous risk evaluation algorithm that is based on collision probabilities between the two AVs. It has been demonstrated how a risk assessment can be used as part of a novel variable trust setting onboard an AV, with the following observations/findings. Increasing the variable trust setting from 0 to 100% (with this reducing the barrier of the virtual boundaries) results in an increased peak risk assessment (PRA) value and

an increased duration of risk imposed (DRI). Based on this initial finding, it is believed the variable trust setting would allow users of an AV to feel more in control (via the variable trust setting knob), allowing the user to explore the technology more (thus, helping to build confidence and better acceptance of the technology), thus allowing for a more comfortable ride through perceived increased safety of AVs

Whilst promising results were obtained, there is scope for much further work. Further work would involve considering a dynamically changing environment to further enhance a realistic approach to the modelling. The use of a high-fidelity proprietary tool such as CarMaker would also be beneficial as it would enable implementing the developed algorithms in real time.

REFERENCES

- Bajpai, J.N. Emerging vehicle technologies & the search for urban mobility solutions, *Urban, Planning and Transport Research*, vol. 4, no. 1, pp. 83–100, 2016.
- D'Souza, J., Burnham, K. J., Pickering, J. E. (2022). Modelling and Simulation of an Autonomous Vehicle Ethical Steering Control System (ESCS). *International Conference on Methods and Models in Automation and Robotics (MMAR)*. Miedzyzdroje: Institute of Electrical and Electronics Engineers (IEEE).
- Geisslinger, M., Poszler, F. and Lienkamp, M., 2023. An ethical trajectory planning algorithm for autonomous vehicles. *Nature Machine Intelligence*, pp.1-8.
- Gilbert, Alex, Dobrila Petrovic, James E. Pickering, and Kevin Warwick. "Multi-attribute decision making on mitigating a collision of an autonomous vehicle on motorways." *Expert Systems with Applications* 171 (2021): 114581.
- Lee, J. and Moray, N., 1992. Trust, control strategies and allocation of function in human-machine systems. *Ergonomics*, 35(10), pp.1243-1270.
- Lee, J.D. and Moray, N., 1994. Trust, self-confidence, and operators' adaptation to automation. *International journal of human-computer studies*, 40(1), pp.153-184.
- Mayer, R.C., Davis, J.H. & Schoorman, F.D. 1995, "An integrative model of organizational trust", *Academy of management review*, vol. 20, no. 3, pp. 709-734.
- Melda Ulusoy (2023). Designing an MPC controller with Simulink (<https://www.mathworks.com/matlabcentral/fileexchange/68992-designing-an-mpc-controller-with-simulink>), MATLAB Central File Exchange. Retrieved February 28, 2023.
- Németh, B., 2023. Coordinated Control Design for Ethical Maneuvering of Autonomous Vehicles. *Energies*, 16(10), p.4254.
- Kalra., N and Paddock, S. M. Driving to safety: How many miles of driving would it take to demonstrate autonomous vehicle reliability? *Transportation*

- Research Part A: Policy and Practice, vol. 94, pp. 182–193, 2016.
- Körber, M., Baseler, E. and Bengler, K., 2018. Introduction matters: Manipulating trust in automation and reliance in automated driving. *Applied ergonomics*, 66, pp.18-31.
- Koopman, P., and Wagner, M. Challenges in autonomous vehicle testing and validation, *SAE International Journal of Transportation Safety*, vol. 4, no. 1, pp. 15–24, 2016.
- Pettersson, I. and Karlsson, I.M. (2015), Setting the stage for autonomous cars: a pilot study of future autonomous driving experiences. *IET Intell. Transp. Syst.*, 9: 694-701. <https://doi.org/10.1049/iet-its.2014.0168>
- Pickering, J. E., and D'Souza, J., 2023. Deontological Ethics for Safe and Ethical Algorithms for Navigation of Autonomous Vehicles (C-NAV) on a Highway. 9TH International Conference on Control, Decision and Information Technologies, July 03 - 06 2023, Rome, Italy.
- Pickering, J.E., Ashman, P., Gilbert, A., Petrovic, D., Warwick, K. and Burnham, K.J., 2018, September. Model-to-decision approach for autonomous vehicle convoy collision ethics. In *2018 UKACC 12th International Conference on Control (CONTROL)* (pp. 301-308). IEEE.
- Rajamani, R., 2011. *Vehicle dynamics and control*. Springer Science Business Media
- Responsible Innovation in Self-Driving Vehicles, 2022. Centre for Data Ethics and Innovation, UK.
- Taiebat, M., and Brown, H. R. Safford, Qu, S., and Xu, M. A review on energy, environmental, and sustainability implications of connected and automated vehicles, *Environmental science & technology*, vol. 52, no. 20, pp. 11 449–11 465, 2018.